Late Neogene evolution of modern deep-dwelling plankton

Flavia Boscolo-Galazzo[1‡*], Amy Jones[2], Tom Dunkley Jones[2], Katherine A. Crichton[1↓], Bridget S. Wade[3], Paul N. Pearson[1]

[1]Cardiff University, School of Earth and Environmental Sciences, Cardiff (UK).

[2]Birmingham University, School of Geography, Earth and Environmental Sciences, Birmingham (UK).

[3]University College London, Department of Earth Sciences, London (UK).

‡Now at Bergen University, Department of Earth Science and Bjerknes Center for Climate Research, Bergen (Norway).

↓Now at Exeter University, Department of Geography, Exeter (UK)

*corresponding author: flavia.boscologalazzo@uib.no

The fossil record of marine microplankton provides insights into the evolutionary drivers which led to the origin of modern deep-water plankton, one of the largest component of ocean biomass. We use global abundance and biogeographic data combined with depth habitat reconstructions to determine the environmental mechanisms behind speciation in two groups of pelagic microfossils over the past 15 million years. We compare our microfossil datasets with water column profiles simulated in an Earth System model. We show that deep-living planktonic foraminiferal (zooplankton) and calcareous nannofossil (mixotroph phytoplankton) species were virtually absent globally during the peak of the middle Miocene warmth. Evolution of deep-dwelling planktonic foraminifera started from subpolar-midlatitude species during late Miocene cooling, via allopatry. Deep-dwelling species subsequently spread towards lower latitudes and further diversified via depth sympatry, establishing modern communities stratified hundreds of meters down the water column. Similarly, sub-euphotic zone specialist calcareous nannofossils become a major component of tropical and sub-tropical assemblages during the latest Miocene to early Pliocene. Our model simulations suggest that increased organic matter and oxygen availability for

27 planktonic foraminifera, and increased nutrients and light penetration for nannoplankton, favored

28 the evolution of new deep water niches. These conditions resulted from global cooling and the

29 associated increase in the efficiency of the biological pump over the last 15 million years.

30 **1. Introduction**

31   The biodiversity of planktonic and nektonic organisms is difficult to explain given the uniform

32 character and vastness of pelagic environments, where genetic isolation seems difficult to maintain

33 (Norris, 2000). Planktonic microorganisms with mineralized shells have often been used as a

34 model to study the mode and tempo of species origination in the open ocean, due to the abundance,

35 widespread distribution, and temporal continuity of their fossil record (e.g., Pearson et al., 1997;

36 Norris, 2000; Bown et al., 2004; Ezard et al., 2011; Norris et al., 2013). Because of the great

37 fossilization potential of their calcium carbonate tests across much of the global ocean, their

38 relatively simple and well-established taxonomy, and highly resolved biostratigraphy, planktonic

39 foraminifera and calcareous nannofossils are amongst the most thoroughly studied best studied

40 fossil groups. Planktonic foraminifera are heterotrophic zooplankton, with different species

41 specialized to feed on different types of food, from other plankton to sinking detritus. In the modern

42 ocean, planktonic foraminifera live stratified across a range of depths spanning from the surface

43 to hundreds of meters down the water column (Rebotim et al., 2017; Meilland et al., 2019).

44 Properties such as food quantity and quality, oxygen, light and pressure all change markedly across

45 the first few hundreds of meters of the ocean. Depending on such down-column variability in

46 environmental conditions, planktonic foraminifera can actively control their living depth of

47 preference, which remains relatively stable during their adult life-stage (Hull et al., 2011; Weiner

48 et al., 2012; Rebotim et al., 2017; Meilland et al., 2019; Duan et al., 2021). A key advantage of

49 using planktonic foraminifera for evolutionary studies is the ability to extract ecological

2

50 information from their shell chemistry. This provides invaluable information about species-

51 specific functional ecology (e.g., feeding strategy) and habitat preferences (e.g., surface versus

52 deep waters), which in combination with biogeographic, taxonomic, biometric, and stratigraphic

53 data have often been used to infer speciation and extinction mechanisms (Norris et al., 1993; Norris

54 et al., 1994; Pearson et al., 1997; Hull and Norris, 2009; Pearson and Coxall, 2012; Woodhouse et

55 al., 2021) and reconstruct phylogenetic relationshipsy (Aze et al., 2011).

56 Calcareous nannoplankton also have a highly resolved and continuous fossil record; they are

57 the most abundant microfossils in oceanic pelagic sediments, and similar to planktonic

58 foraminifera, their spatial distribution ranges from tropical to subpolar latitudes (Poulton et al.

59 2017). In the modern ocean they also live stratified in the water column, with species adapted to

60 euphotic waters, and species adapted to live deeper (Poulton et al., 2017). In contrast to planktonic

61 foraminifera, nannoplankton are predominantly autotrophic, performing photosynthesis in water

62 where light penetration is sufficient, although there is evidence for heterotrophy (mixotrophic

63 behavior) in some extant (Godrjian et al., 2020) and fossil (Gibbs et al., 2020) species. In euphotic

64 waters, organic matter production from nannoplankton is at the base of pelagic food chains and of

65 the functioning of the ocean biological carbon pump. Taxonomic, biometric and stratigraphic data

66 have been used to establish phylogenetic relationships between fossil nannoplankton species

67 (Young and Bown, 1997).

68 Little emphasis has been given to the long-term drivers of evolutionary patterns observed in

69 fossil plankton from species to phylum level, although more recently, a broad connection with

70 changing climate and ocean properties has been suggested (e.g., Ezard et al., 2011; Norris et al.,

71 2013; Frass et al., 2015; Henderiks et al., 2020; Lowery et al., 2020). Boscolo-Galazzo, Crichton

72 et al. (2021) showed that over the last 15 million years the remineralization of particulate organic

73   carbon (POC) in surface waters declined markedly driven by climate and ocean cooling (Kennett

74   and Von der Borch, 1985; Kennett and Exon, 2004; Cramer et al., 2011; Zhang et al., 2014; Herbert

75   et al., 2016; Sosdian et al., 2018; Super et al., 2020), increasing the efficiency of the ocean

76   biological pump in delivering organic matter at depth. Such a mechanism was key to promote the

77   evolution of life in deep waters, allowing the development of the modern twilight zone ecosystem

78   (Boscolo-Galazzo, Crichton et al., 2021). The goal of this study is to combine the fossil record of

79   two ecologically complementary calcareous microplankton groups seldom analyzed together,

80   planktonic foraminifera and nannoplankton, and together with model simulations, help disentangle

81   the evolutionary drivers of modern deep-dwelling plankton. We use the planktonic foraminiferal

82   dataset from Boscolo-Galazzo, Crichton et al. (2021) and extend our analysis to calcareous

83   nannofossils in coeval sediment samples to assess their abundance and distribution pattern. We

84   compare the results from these two groups and contrast them against time and site-specific model

85   water column profiles for POC and oxygen (O_2) obtained from the cGENIE Earth System model.

86   Further, using stable isotopes, depth habitat reconstructions, abundance and biogeography data we

87   reconstruct the speciation mechanisms which led to the evolution of modern deep-dwelling

88   planktonic foraminiferal species.

89

90   **2. Methods**

91   **2.1 Planktonic foraminifera**

92   In this study we focus on the deep-dwelling groups of macroperforate planktonic foraminifera

93   of the hirsutellids, globorotaliids, truncorotaliids and globoconellids, which in the modern ocean

94   calcify and live mostly in the twilight zone of the ocean, i.e. between 200-1000 m (Birch et al.,

4
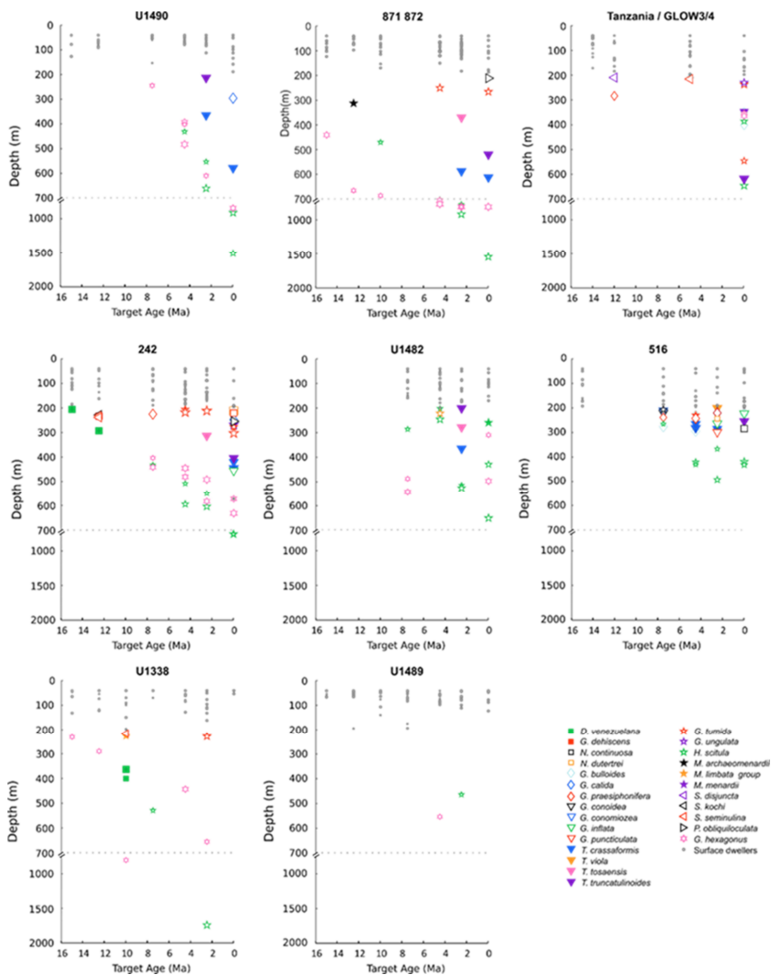
Figure 1. Depth-habitat reconstructions for middle Miocene to present planktonic foraminiferal species at the investigated sites. Surface dwellers (species living at depths shallower than 200 m) are indicated with a grey dot, deeper species are indicated with colored symbols. Relative size of symbols represents the size fractions of the sample. Reproduced from Boscolo-Galazzo, Crichton et al. (2021).

102 2012; Rebotim et al., 2017), and have a more complete fossil record than deep-dwelling

103 microperforate planktonic foraminifera (Kennett and Srinivasan, 1983).

104 Planktonic foraminiferal data and depth habitat reconstructions (Fig. 1) are from Boscolo-

105 Galazzo, Crichton et al. (2021). They were obtained from globally and latitudinally distributed

106 DSDP (Deep Sea Drilling Project)/ODP (Ocean Drilling Program)/IODP (Integrated Ocean

107 Drilling Program & International Ocean Discovery Program) sites and from cores drilled onshore

108 and offshore Tanzania, all characterized by abundant calcareous microfossils (Boscolo-Galazzo,

109 Crichton et al., 2021). The work was focused on seven target ages (15 Ma, 12.5 Ma, 10 Ma, 7.5

110 Ma, 4.5 Ma, 2.5 Ma, 0 Ma/Holocene). To avoid sample-aliasing, bulk sediment stable isotopes

111 were measured on an average of ten samples per target age at each site. The sample displaying

112 mean oxygen stable isotope values was chosen for subsequent analyses (Boscolo-Galazzo,

113 Crichton et al., 2021). Taxonomy follows: Berggren (1977), Kennett and Srinivasan (1983), Bolli

114 et al. (1989), Scott et al. (1990), Berggren (1992), Pearson (1995), Majewski (2010), Fox and

115 Wade (2013), Spezzaferri et al. (2015), Wade et al. (2018), Lam and Leckie, (2020a), with

116 phylogenetic genus names from Aze et al. (2011).

117 Ages were determined based on biostratigraphic analysis mostly following the biozonation

118 scheme by Wade et al. (2011).

119 Foraminiferal picking for stable isotope measurements were conducted from the size fractions:

120 180-250 µm, 250-300 µm, 300-355 µm (Boscolo-Galazzo, Crichton et al., 2021). Stable isotopes

121 were measured on an average of 15 different species per sample, using ~25 specimens for common

122 species, and as many specimens as possible for rare species. Stable isotopes were measured at

123 Cardiff University. Stable isotope results are shown in FigsFig. S1 to S9 in the Supplement. Only

124 data from the largest of the three measured size fractions are shown when data from more than one

6

Formatted: English (United States)

Formatted: English (United States)

125 size fraction are available. Data from size fractions other than those above are shown only when a

126 species did not occur within the preferred size interval. Foraminiferal abundance counts were

127 carried out in two size fractions, 180-250 μm and >250 μm, counting up to 300 specimens in each.

128 Total abundances were derived by summing up abundances from these two size fractions.

129   Boscolo-Galazzo, Crichton et al. (2021) reconstructed planktonic foraminiferal depth habitat

130 (Fig. 1) using a combined model-data approach, solving the paleotemperature equation of Kim and

131 O'Neill (1997) for each data point using measured foraminiferal δ^{18}O, global ice volume estimates,

132 and the cGENIE modeled salinity field to determine local water δ^{18}O, and then use the model

133 temperature-depth curve to determine depth. The full method is described in Boscolo-Galazzo,

134 Crichton et al. (2021).

135

136 **2.2 Calcareous Nannofossils**

137 Quantitative calcareous nannofossil data were collected from the same samples as used for

138 planktonic foraminiferal analysis or, when this was not possible, stratigraphically adjacent samples

139 (Table S1 in the Supplement). A cascading count technique was used to maximise nannofossil

140 diversity recovery and quantification of low abundance species (Styzen, 1997). Nannofossils were

141 counted per field of view (FOV) until a minimum of 400 specimens were achieved for each sample.

142 However, if a high abundance species exceeded an average of 25 specimens per FOV, it was

143 excluded from subsequent counts in that sample and its abundance scaled-up based on its average

144 abundance and the total numbers of FOV counted. Only specimens directly counted contributed

145 to the minimum count threshold of 400 specimens. An additional scan of two slide transects were

146 undertaken to record rare species not observed during the extended count and are included in the

147 total species richness and diversity analyses. Samples for nannofossil analysis were prepared using

7

148 the smear slide technique (Bown & Young, 1998). Calcareous nannofossils were observed using

149 both plane-polarised (PPL) and cross-polarised light (XPL) on a Zeiss Axioscope light-microscope

150 at x1000 magnification. Identification and taxonomy used herein follows Young et al. (1997) and

151 is coherent with the recent Neogene calcareous nannofossil taxonomy (Ciummelli et al., 2016;

152 Bergen et al., 2017; Blair et al., 2017; Boesiger et al., 2017; Browning et al., 2017; de Kaenel et

153 al., 2017).

154 **2.3 Plankton Ecogroups**

155 In order to compare the datasets obtained from the planktonic foraminiferal and nannofossil

156 analysis, we grouped species into ecogroups based on depth-habitat preferences. Planktonic

157 foraminiferal ecogroups are defined based on paleodepth habitat reconstructions from Boscolo-

158 Galazzo, Crichton et al. (2021): the euphotic zone ecogroups includes species with an average

159 depth habitat shallower than 200 m (the bottom of the euphotic zone), the twilight zone ecogroup

160 includes species with an average depth habitat coinciding with the twilight zone (200-1000 m).

161 The twilight zone ecogroup is largely composed of species within the globoconellids, the

162 *Globorotalia merotumida-tumida* lineage, the hirsutellids and the truncorotaliids, but also includes

163 species from other genera, such as *Globigerinella calida*, *Globorotaloides hexagonus*, *G.*

164 *variabilis*, and *Pulleniatina obliquiloculata*. *Dentoglobigerina venezuelana* has a changeable

165 depth habitat through time (see discussion in Matsui et al., 2016; Wade et al., 2018); following the

166 depth habitat reconstructions from Boscolo-Galazzo, Crichton et al., (2021) it was grouped as

167 euphotic zone species for target ages 15, 12.5, 7.5, 4.5 Ma and as twilight zone species for target

168 age 10 Ma. Species were excluded from the grouping when they are known to have a marked

169 seasonality in abundance and depth habitat (*Globigerina bulloides, Globigerinella*

170   *praesiphonifera* and the neogloboquadrinids) (e.g., Jonkers and Kucera, 2015; Greco et al., 2019),

171   and if they were too rare and depth habitat reconstruction was not possible (*Candeina nitida*).

172   Three ecogroups for calcareous nannofossils are used: upper-euphotic, lower-euphotic and

173   sub-euphotic. The upper-euphotic group is represented by: *Discoaster* spp., *Rhabdosphaera*

174   *xiphos*, *Reticulofenestra* spp. and *Gephyrocapsa* spp. (excluding *G. ericsonii*); the lower-euphotic

175   ecogroup contains: *Rhabdosphaera clavigera, Gephyrocapsa ericsonii* and *Ceratolithus* spp.,

176   finally the subeuphotic ecogroup includes: *Florisphaera profunda* and *Calciosolena murrayi*.

177   Because species specific stable isotope measurements and depth habitat reconstructions are

178   difficult for calcareous nannofossils, species depth-habitat preference was assigned based on the

179   literature (Poulton et al., 2017; Tangunan et al., 2018). In particular, Poulton et al. (2017) described

180   vertically separated coccolithophores communities sampled during a meridional cruise in the

181   Atlantic Ocean. Here we use their criteria for assigning nannofossil species into ecogroups,

182   whereby in the upper-euphotic zone ecogroup we include species found to live in waters with

183   >10% surface irradiance, in the lower-euphotic zone ecogroup we group species found to live in

184   waters with 10-1% irradiance, and in the sub-euphotic zone ecogroup we group species found to

185   live in waters with <1%, i.e. too low to support photosynthesis (Poulton et al., 2017). *Discoaster*

186   become extinct in the early Pleistocene, therefore, its depth habitat remains under debate as the

187   group has no extant relative (Schueth and Bralower, 2015; Tangunan et al., 2018). However,

188   geochemical evidence from oxygen isotope values of *Discoaster* and planktonic foraminifera

189   (*Globorotalia menardii*, *Dentoglobigerina altispira* and *Globigerinoides obliquus*), reveal

190   comparable values and signifies that *Discoaster* likely inhabited the upper euphotic zone

191   (Minoletti et al., 2001).

9

192   For each target age, the relative abundance of ecogroups was calculated summing up the

193   abundance counts of all the individual species pertaining to an ecogroup at each site, hence,

194   ecogroup abundance data represent global mean values. For both nannofossils and planktonic

195   foraminifera, the percentage of each ecogroup per time bin was converted into pie-charts (FigsFig.

196   2-5). Diversity indexes for both foraminiferal and nannofossil ecogroup were calculated using the

197   statistical software Past (Hammer et al., 2001) (Fig. 6).

198
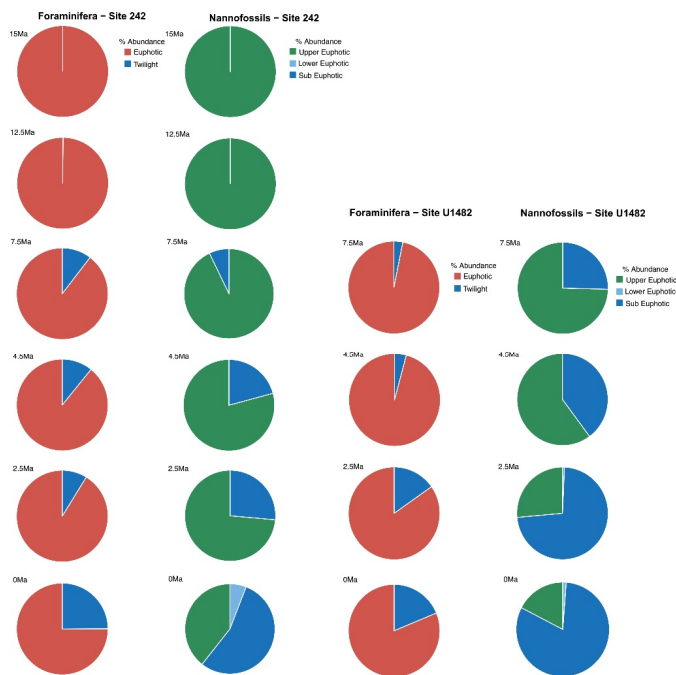
199

200   **Figure 2.** Foraminiferal and nannofossil ecogroup abundance at Site 242 and U1482.

201

202

2.4 cGENIE model

We extracted model output for Particulate Organic Carbon (POC) and oxygen concentration from the cGENIE simulations for each of the seven target ages as described fully in Boscolo-Galazzo, Crichton et al. (2021). To facilitate a general discussion of near-surface changes, we divided the data latitudinally by calculating the arithmetic mean for low latitudes (<16° latitude), two mid-latitude bands (mid 1: 16° to 40°, mid 2: 40° to 56°) and high latitudes (>56°). The cGENIE simulations take account of changing boundary conditions including CO_2 forcing, bathymetry and ocean circulation (Crichton et al., 2020). The model's ocean biological carbon pump is temperature dependent, where temperature affects both nutrient uptake rates at the surface and remineralization rates of sinking particulate organic matter down the water column (Crichton et al., 2021).

3. Results

3.1 Plankton Ecogroups

For both calcareous nannoplankton and planktonic foraminifera, the variation in abundance of euphotic zone and deeper-dwelling ecogroups show global patterns recognised across sites. Additionally both group indicate a long-term directionality towards increased abundance of deep-dwelling ecotypes. Among planktonic foraminifera, the twilight zone ecogroup increases in abundance through time starting at 7.5 Ma (Fig. 6). The relative abundance of the twilight zone ecogroup in the middle Miocene is 15% and it increases to ~30% in the Holocene time slice (Fig. 6). The average abundance of the euphotic zone species ecogroup in the middle Miocene is 85% and it decreases through time until reaching 60% in the Holocene (Fig. 6). In the twilight zone ecogroup we observe an increase in the total number of species from about 1-2 species at 15 Ma, to 14 species in the Holocene (Fig. 6). In the middle Miocene this group comprised 1/6 of the total

226 number of species in our samples, while in the Holocene it represents almost the half. All the

227 diversity indexes show a late Miocene to Holocene increasing trend for the twilight zone ecogroup

228 (Fig. 6).

229   Calcareous nannofossil assemblages are dominated by the upper-euphotic ecogroup from

230 15 to 10 Ma at all sites (~~Figs~~Fig. 2-5). At 7.5 Ma the sub-euphotic ecogroup first becomes a

231 significant component of assemblages at Indian Ocean sub-tropical Sites U1482 and to some extent

232 Site 242, but it is not until the 4.5 Ma time slice that the sub-euphotic ecogroup becomes a

233 significant component of assemblages at the majority of locations (Sites 516, 871/872, 242, U1338,

234 U1482, U1489; ~~Figs~~Fig. 2-5). By the Holocene time slice, coccoliths of sub-euphotic species are

235 dominant at most locations, except at Eastern Equatorial Pacific Site U1338 (~~Figs~~Fig. 6 and 4). At

236 the southern high latitude Site 1138 there is no significant contribution from coccoliths of either

237 lower-euphotic or sub-euphotic species at any point, although there is no data from the Pliocene

238 to Holocene time slices at this location (Fig. 5). Global average compositions of calcareous

239 nannofossil assemblages reflect the changes noted above, with a marked and rapid decline in the

240 relative contribution of the upper-euphotic ecogroup, and a corresponding increase in the sub-

241 euphotic zone ecogroup through the Pliocene and to Holocene (Fig. 6).

242 **3.2 Planktonic foraminiferal deep-dwelling species: depth habitat, abundance and**

243 **biogeography**

244 **3.2.1 Hirsutellids**

245 The only hirsutellid species occurring in our Miocene samples is *Hirsutella scitula*. At 15 Ma this

246 morphospecies is common only at Site 1138 (~8%), sporadically occurs at Site 516 (<1%) and is

247 absent at the other investigated sites (~~Figs~~Fig. 7). Oxygen isotopes range from 0.5 to 1.3‰

248 (~~Figs~~Fig. S1-

249
250
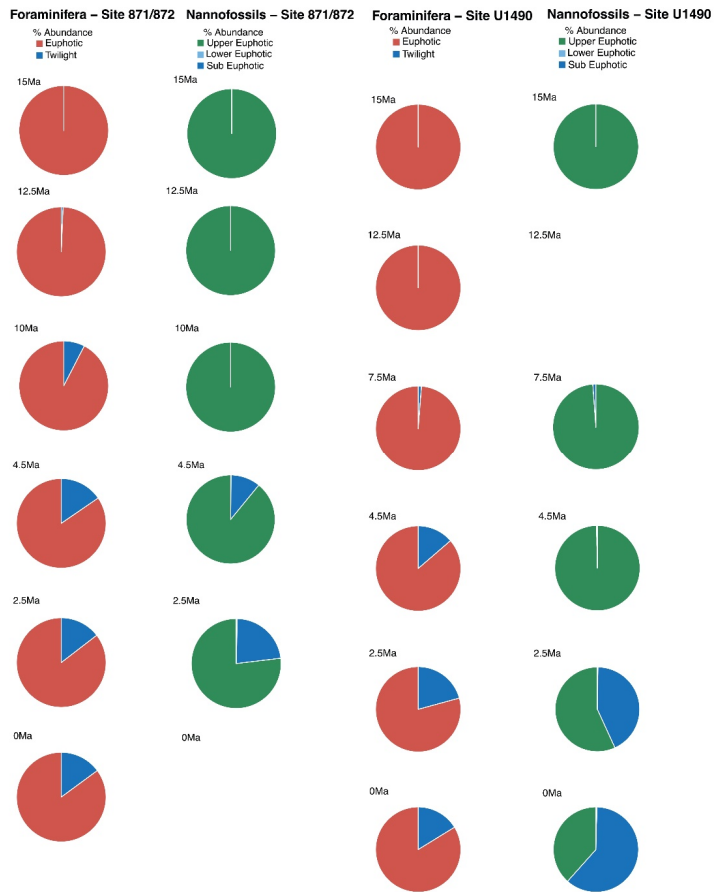
Figure 3. Foraminiferal and nannofossil ecogroup abundance at Site 871/872 and U1490.

251

252

253

254

255

256

257

258   S2). Depth-habitat reconstructions for Site 1138 are unattainable from $\delta^{18}O$ data due to the

259   overprinting effect of subpolar front shifts at this location, but habitat reconstruction at Site 516

260   suggests a paleodepth habitat shallower than 200 m. By 12.5 Ma, *H. scitula* appears at Site U1338

261   and U1489 in very low abundance (<0.5%) (Fig. 7). At Site U1489 the species was so rare that it

262   was encountered when picking for stable isotopes and no more when counting for species

263   abundances, despite the use of different splits of the residue. No differences were observed

264   between 12.5 and 10 Ma in the biogeography of *H. scitula* (Fig. 7). However, by 7.5 Ma, *H. scitula*

265   occurs at all our low latitude sites (Fig. 8) with oxygen isotopes ranging from -0.5 to 2.0‰

266   (~~Figs~~Fig. S3-S9), which according to depth habitat reconstructions translates to 250 and 500 m

267   water depth (Boscolo-Galazzo, Crichton et al., 2021). This is similar to that of *Globorotaloides*

268   *hexagonus* (Fig. 1), the only twilight zone dweller we observed at tropical sites at 15 Ma,

269   displaying stable isotopes ranging from 0 to 1‰, which translates to depths around 300-500 m. In

270   the late middle Miocene the stable isotope values of *G. hexagonus* increase to 2-2.5‰ (~~Figs~~Fig.

271   S3-S9). Similarly, the oxygen isotope values of tropical *H. scitula* increased through time, reaching

272   2-3‰ in the youngest target ages. In line with this, the reconstructed depth habitat of *H. scitula*

273   and *G. hexagonus* increases through time in a stepwise fashion, and in the Holocene it reaches

274   down to 800-1500 m (Fig. 1) (Boscolo-Galazzo, Crichton et al., 2021). *Hirsutella scitula* becomes

275   gradually more common at low latitude sites through the Miocene-Pliocene, although it never

276   becomes abundant. In our record, *Hirsutella margaritae* and *H. theyeri* first appear in the early

277   Pliocene at a depth between 200-300 m (Fig. 1) (oxygen isotopes range -1 to -0.5‰), similar to

278   that of *H. hirsuta* (oxygen isotopes range 0 to 1‰) when it first appears in the Holocene (~~Figs~~Fig.

279   S3-S9).

280

281
282
283
284   **Figure 4.** Foraminiferal and nannofossil ecogroup abundance at Site U1338 and U1489.
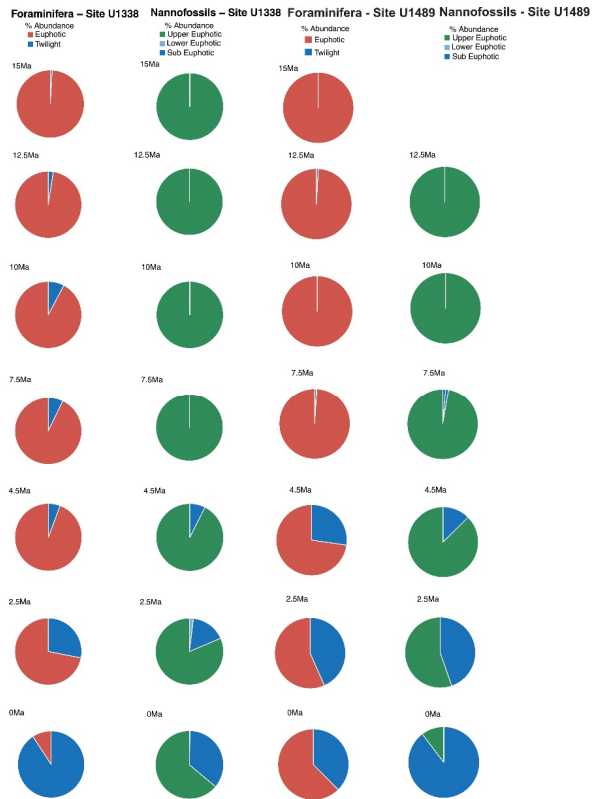
285
286
287
288
289
290
291

3.2.2 Truncorotaliids

The earliest appearances of *Truncorotalia crassaformis* in our record corresponds to our 4.5 Ma time slice at Site 1138 in the Indian Ocean sector of the Southern Ocean where it represents >20% of the assemblage, and in coeval sediments at mid-latitude Site 516 in the southwest Atlantic, where it represents ~9% of the assemblage (Fig. 9), with oxygen isotopes ranging from 1.5 to 3.0‰ (~~Figs~~Fig. S1-S2). At Site 516 we observe the co-occurrence of *T. oceanica* (~14%) and *T. crassaformis* in the early Pliocene (4.5 Ma), and of *T. viola* (~5%) and *T. crassaformis* (~13%) in the late Pliocene (2.5 Ma) (Fig. 10). We did not observe *T. oceanica* and *T. viola* anywhere else. *T. oceanica* and *T. crassaformis* display almost overlapping $\delta^{18}O$ values and depth habitat (Fig. S2) but *T. crassaformis* has 0.5‰ lower $\delta^{13}C$ values. Oxygen stable isotope data (1‰; Fig. S2) and habitat reconstructions for Site 516 indicate that a subsurface habitat (>200 m) was already occupied by *T. crassaformis* at the beginning of its evolutionary history (Fig. 1). The late Pliocene appearance of *T. viola* at Site 516, which differs from *T. crassaformis* in having a more convex umbilical side, a triangular outline and a subacute profile, is associated with a shift to more positive oxygen isotope values of *T. crassaformis* (1.5‰) and to slightly greater depths (Fig. 1).

We find *T. crassaformis* by the late Pliocene at our investigated tropical and subtropical sites (2.5 Ma, Site U1338, U1489, 872, U1490, 242, U1482) (~~Figs~~Fig. 10-11), with oxygen isotope values ranging from 1.0 to 2.0‰ which translate to depth habitats of 400-600 m (Boscolo-Galazzo, Crichton et al., 2021; Fig.1). The appearance of *T. crassaformis* at our low latitude sites is coeval with the appearance in our record of *Truncorotalia tosaensis*, morphologically transitional between *T. crassaformis* and *T. truncatulinoides* (Lazarus et al., 1995) (Fig. 10). *Truncorotalia tosaensis* displays oxygen isotopes values ranging from 0 to 0.5‰ (~~Figs~~Fig. S1-S9), which translate to 300-350 m depth (Fig. 1). Consistent with earlier findings (Jenkins and Srinivasan
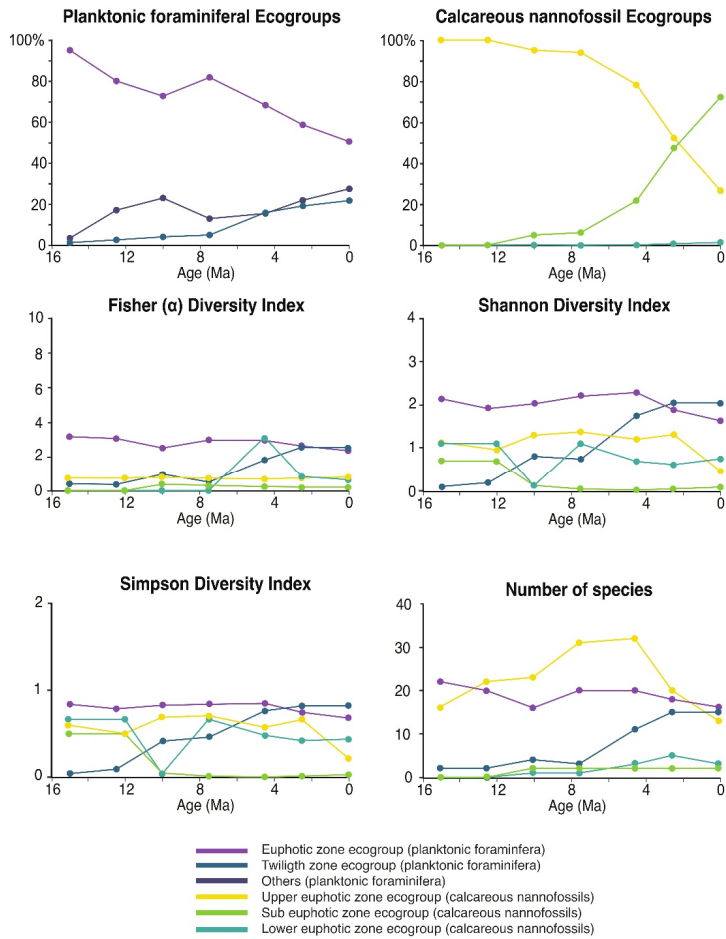
16

315 1986; Lam and Leckie 2020b; Lazarus et al., 1995), we record the first occurrence of *T.*

316 *truncatulinoides* in the late Pliocene in the south-west Pacific (2.5 Ma, Site U1482), and only later

317 in the North Pacific (0 Ma, Site 872), Indian Ocean (0 Ma, Site 242) and South Atlantic (0 Ma,

318 Site 516) (Fig. 11). *Truncorotalia truncatulinoides* records oxygen isotope values ranging from -

319 1 to 2‰, more negative than coeval *T. crassaformis* (FigsFig. S3-S9). *Truncorotalia*

320 *truncatulinoides*, although reported in the modern tropical ocean as one of the species living at the

321 greatest depths, occupies a shallower depth habitat than *T. crassaformis* when it first appears in

322 our tropical to subtropical records (2.5 Ma).

323
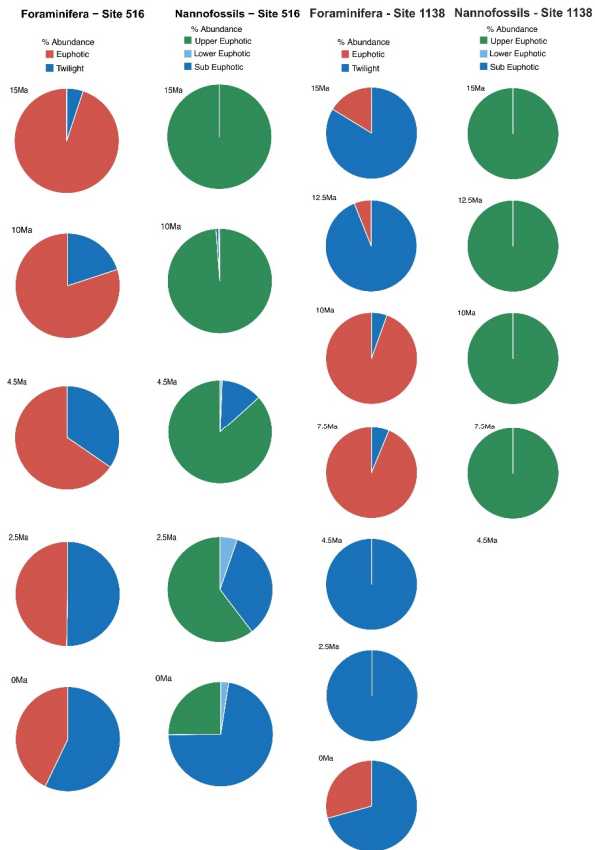
Figure 5. Foraminiferal and nannofossil ecogroup abundance at Site 516 and 1138.

324

325

326

327

328

Planktonic foraminiferal Ecogroups

Calcareous nannofossil Ecogroups

Fisher (α) Diversity Index

Shannon Diversity Index

Simpson Diversity Index

Number of species

Euphotic zone ecogroup (planktonic foraminfera)
Twiligth zone ecogroup (planktonic foraminifera)
Others (planktonic foraminifera)
Upper euphotic zone ecogroup (calcareous nannofossils)
Sub euphotic zone ecogroup (calcareous nannofossils)
Lower euphotic zone ecogroup (calcareous nannofossils)

329

Figure 6. Planktonic foraminiferal and nannofossil ecogroups relative abundance and diversity

indexes.

332

333

334

335

19

3.2.3 Globorotaliids

336

337 With globorotaliids here we refer to the *Globorotalia merotumida-tumida* lineage composed by *G.*

338 *merotumida*, *G. pleosiotumida*, *G. tumida* and *G. ungulata* (Kennett and Srinivasan, 1983). This

339 group first appears with *Globorotalia plesiotumida* in our 10 Ma time slice at Site 871 (Fig. 7). At

340 all the investigated low latitude sites, we find *G. tumida* by 4.5 Ma with abundances between 2-

341 24% (Fig. 9). *Globorotalia plesiotumida* co-occurs with *G. tumida* only at Sites 872 and 242

342 corresponding to our 4.5 Ma time slice (Fig. 9; Fig. S9). In our records, *G. tumida* consistently

343 displays oxygen isotope values between -1 to 0‰ (~~Figs~~Fig. S3-S9), and an average depth habitat

344 around 250 m, with a shallowest occurrence at 50 m and a deepest occurrence around 600 m (Fig.

345 1). Similar oxygen isotope values and depth habitat preference are recorded for *G. plesiotumida*

346 and *G. ungulata* (Fig. 1 and ~~Figs~~Fig. S3-S9).

3.2.4 Globoconellids

347

348 In our records, *Globoconella miozea* is a dominant component of planktonic foraminiferal

349 assemblage at Site 1138 at 15 Ma (65%) and occurs in moderate abundance at Site 516 (5%) (Fig.

350 7). The distribution of globoconellids appears restricted to southern high to mid-latitudes during

351 the middle Miocene and the late Miocene to Pliocene. At Site 1138 globoconellids decrease in

352 abundance through time, with *Globoconella panda* the only late Miocene (7.5 Ma) species (<1%;

353 with δ^{18}O of 3‰), followed only by *Globoconella inflata* in the Holocene (4.2%; with δ^{18}O of

354 3.5‰) (Fig. 11). On the contrary, at Site 516 globoconellids increase in abundance through time

355 becoming a characteristic feature of the planktonic foraminifera assemblage as noted in previous

356 studies of this area (Berggren, 1977; Norris et al., 1994) (~~Figs~~Fig. 7-11). In the Holocene *G. inflata*

357 is most abundant at mid-latitude Site 516 (22.7%; with δ^{18}O of 1‰), but also occurs in the

358 subtropical (<0.5%; with δ^{18}O of 0.9‰) and subpolar Indian ocean (4.2%; with δ^{18}O of 3.5‰)

20

359 (Fig. 11; ~~Figs~~Fig. S1-S3). Depth habitat reconstructions for the globoconellids show a deepening

360 trend through time although less marked compared to those of other deep-dwelling groups

361 considered in this study (Boscolo-Galazzo, Crichton et al., 2021; Fig. 1). At Site 516, the depth

362 habitat is just above 200 m for middle Miocene *Globoconella miozea* (δ^{18}O 0.9‰), just below 200

363 m for late Miocene *G.* ~~conoidea~~miotumida and *G. conomiozea* (δ^{18}O 1‰), and around 350 m for

364 late Pliocene *Globoconella puncticulata* (δ^{18}O 1.6‰) the precursor of *G. inflata,* which shows a

365 similar depth habitat at this site (δ^{18}O 1-1.2‰; Fig. S2), (Fig. 1). At Site 242 the average depth

366 reconstruction for the Holocene *G. inflata* is of ~450 m (δ^{18}O 0.9‰; Fig. S3), similar to that of *T.*

367 *crassaformis* and *T. truncatulinoides* (Boscolo-Galazzo, Crichton et al., 2021; Fig. 1).

368 **4. Discussion**

369 **4.1 Evolution of a deep-plankton ecological niche linked to late Neogene cooling**

370 We observe a trend of increasing ecological importance of deep-dwelling species in both

371 calcareous nannofossil and foraminiferal communities from the late Miocene to Recent. The

372 foraminiferal twilight zone ecogroup shows a marked increase in abundance and diversity at 7.5

373 Ma, at the same time as the first significant appearance of the sub-euphotic ecogroup within

374 coccolithophore assemblages, and coinciding with a possible acceleration of global cooling

375 (Cramer et al., 2011; Crichton et al., 2020). Fossil deep-dwelling coccoliths are dominated by one

376 species, *Florisphaera profunda,* which is often very abundant in Plio-Pleistocene sediments. This

377 makes our sub-euphotic ecogroup a low diversity – high abundance assemblage, whose origin

378 significantly impacts the relative abundance balance between ecogroups, but with little change in

379 diversity metrics towards the modern. Although there are morphological variants of *F. profunda*

380 in the modern oceans, potentially representing sub-species or pseudo-cryptic species (Quinn et al.,

381 2005), these are not distinguished in fossil assemblages and documenting their divergence times

21

382   requires either further molecular genetic or detailed morphological analyses. The one clear signal

383   in our diversity analyses is a late Miocene – early Pliocene peak in upper-euphotic species richness,

384   followed by a marked decline through the late Pliocene to the Holocene. The late Miocene-

385   Pliocene peak diversity is present in previous global compilations of total nannofossil diversity

386   (Bown et al. 2004; Lowery et al. 2020), but here we show that this signal is driven by first a

387   diversification and then progressive extinction almost entirely within upper-euphotic taxa.

388   Modern planktonic foraminifera evolved in two main diversification pulses in the middle Miocene

389   (16-14 Ma) and during the late Miocene-Pliocene transition (6-4.5 Ma) (Kennett and Srinivasan,

390   1983; Kucera and Schönfeld, 2007). Our species abundance and diversity data show that this

391   diversification was mostly driven by the origin of lineages of deep/subsurface dwelling species

392   (~~Figs~~Fig. 7-11 and Fig. 6). Diversity among euphotic zone species remained constant from the

393   middle Miocene to the early Pliocene, then declined (Fig. 6). This pattern, similar to calcareous

394   nannofossils, may explain early records pointing to a decrease in Pliocene to Recent planktonic

395   foraminiferal diversity (Wei and Kennett, 1986).

396   The observed evolutionary patterns in planktonic foraminifera and coccolithophores can

397   be explained by the development of environmental conditions favourable to deep living plankton
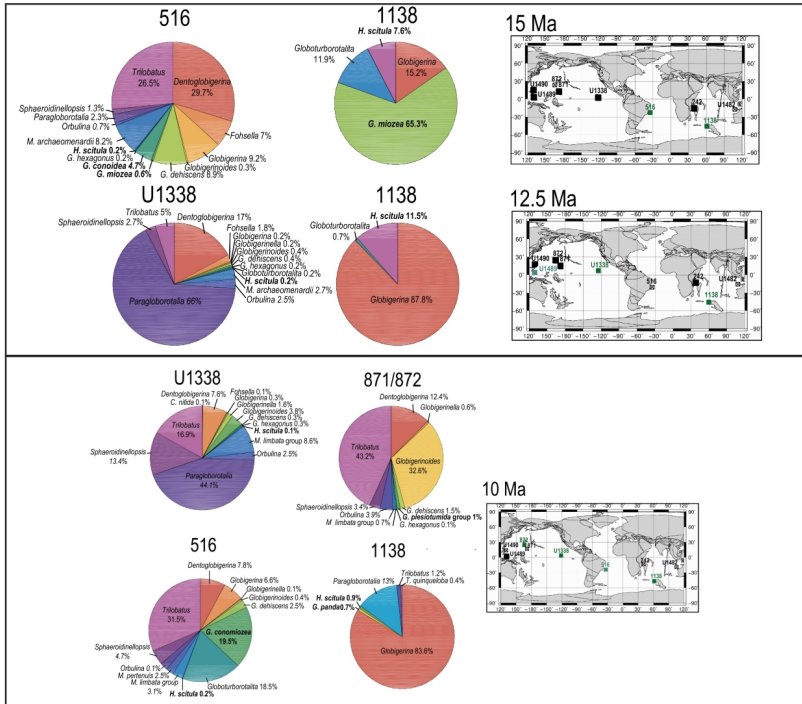
Figure 7. Abundance and biogeography of planktonic foraminiferal species at 15, 12.5, and 10 Ma. In the pie-charts twilight zone planktonic foraminiferal species are in bold. Sites where twilight zone planktonic foraminifera were found are highlighted in green in the maps. The crossed square symbol in the maps indicate that the time interval of interest was not recovered for a given site. Continental configuration follows: Ocean Drilling Stratigraphic Network (GEOMAR, Kiel, Germany).

with cooling. For the deep-dwelling planktonic foraminifera, survival requires the availability of food at depth, and with the exception of few species adapted to oxygen minimum zones (Davis et al., 2021), the absence of severe oxygen depletion. In the published literature there is a general tendency for planktonic foraminiferal $\delta^{18}O$ values to be tightly grouped during times of warm climate, becoming more spread-out during cooling episodes, for instance the transition from mid- to late Cretaceous (Ando et al., 2010) and early to middle Eocene (John et al., 2013). In light of our findings such tight $\delta^{18}O$ values, may indicate times when food and oxygen availability at depth were limited, allowing planktonic foraminifera to live at shallower depths only. Because our data are restricted to certain time slices and locations, we only capture a part of the overall pattern for the Neogene, but other examples of depth-related evolution in the Neogene include the *Fohsella peripheroronda – F. fohsi* lineage in the middle Miocene (Hodell and Vayavananda, 1993; Norris et al., 1993) and the appearance of various deep-dwelling digitate species in the Plio-Pleistocene (Coxall et al., 2007).

Deep-dwelling coccolithophores, most notably *Florisphaera profunda*, require dissolved macronutrients (N, P) and at least some degree of light penetration (Quinn et al., 2005; Poulton et al., 2017). The requirement for light penetration to depth is most clearly shown by the absence of *F. profunda* beneath high surface productivity regions where nutrients are not limited at depth but light is rapidly attenuated by more abundant mixed layer microplankton (Beaufort et al., 1999). For coccolithophores, the cooling-driven shift from nutrient recycling within to below the mixed layer, may have provided the ecological driver for species to live in deeper, more nutrient-rich waters, but, as mixed layer waters cleared, also allowed the irradiance necessary for photosynthesis to penetrate to these new deeper habitats. Additionally, the capability of coccolithophores to absorb

24

432 carbon and nutrients from seawater under low light conditions (Godrjian et al., 2020; 2021) may

433 have also aided in the occupation of new deep water niches.

434   Our model outputs from cGENIE is consistent with this interpretation, organic matter

435 export (POC at 40 m in Fig. 12) reduced with cooling, suggesting an overall decrease in primary

436 productivity at all 4 latitudinal bands considered in this study. Fewer particles in surface waters

437 would have allowed greater light penetration (Fig. 12), at the same time, the model indicates

438 enhanced organic matter delivery at >200 m with cooling. Greater organic matter delivery below

439 the euphotic zone, suggests a deeper remineralization depth and increased dissolved nutrients

440 availability at depth. This is most clearly shown in the modelled low and mid latitudes near-surface

441 waters. Oxygen availability also increased, particularly below 100 m depth in low latitudes and

442 further down the water column, below 200 m depth (Fig. 12).

443   Nonetheless, planktonic foraminifera and nannoplankton have distinct trophic statuses

444 (zoo- versus phytoplankton), further coccolithophore species require light for their dominantly

445 photosynthetic mode of life. In our data, such differences between the requirements of zoo- and

446 phytoplankton deep-dwellers is clearly observed in the biogeographic patterns. Sub-euphotic

447 coccolithophores are consistently more abundant in low nutrient sub-tropical locations (e.g. DSDP

448 Site 242 and IODP Site U1482; Fig. 2). The end-member of this biogeographic difference is ODP

449 Site 1138, in the Southern Ocean. Here, twilight foraminifera dominate most time intervals,

450 presumably due to high export production. However, lower-euphotic and sub-euphotic

451 coccolithophores are effectively excluded, due to turbid, high-productivity surface waters (Fig. 5).

452 This pattern is also supported through a comparison of high to low productivity tropical sites in

453 the Holocene – the Eastern Equatorial Pacific Site U1338 has abundant twilight foraminifera, but

454 relatively low abundances of sub-euphotic coccolithorestaxa (Fig. 4), whereas the more

oligotrophic Site U1482 (Fig. 2) has lower abundances of twilight foraminifera and higher abundances of sub-euphotic coccolithophores.

Despite these ecological differences between zoo- and phytoplankton, we suggest there is a shared environmental driver for the evolution of deep-dwelling coccolithophores and planktonic foraminifera linking the evolution of deep-dwelling specialists in each group. Efficient near-surface recycling of organic carbon in past warm climates, such as the middle Miocene (Fig. 12), precluded the occupation of the deep habitat for both groups by reducing both organic carbon transfer (food limitation for foraminifera and for foraminiferal prays such copepods) and light penetration (photosynthesis for coccolithophores) to depth (Fig. 2-6). Global cooling since the middle Miocene (Kennett and Von der Borch, 1985; Kennett and Exon, 2004; Cramer et al., 2011; Zhang et al., 2014; Herbert et al., 2016; Sosdian et al., 2018; Super et al., 2020), however, led to a decreased export of organic matter and a deepening of the mean organic matter remineralization depth, which in turn favoured the evolution of deep water niches in planktonic foraminifera (Fig. 1) and nannoplankton via increased availability of organic matter, oxygen, and likely nutrients at depth (Fig. 12), and clearing of surface waters.

### 4.2 Mechanisms of speciation of deep-dwelling planktonic foraminifera

The hirsutellids gave rise to a large late Neogene radiation among planktonic foraminifera, leading to the origin of modern phyletic groups such as the menardellids, globoconellids, truncorotaliids, and the globorotaliids of the *Globorotalia merotumida - tumida* lineage (Kennett and Srinivasan, 1983; Scott et al., 1986; Aze et al., 2011). The majority of the modern representatives of these groups are lower euphotic zone to twilight zone species. The hirsutellids originated about 18 Ma (Wade et al., 2011) from *Globorotalia zealandica* (Kennett and Srinivasan,

478 1983), the first representative of the group being *Hirsutella praescitula* (Kennett and Srinivasan,

479 1983; Aze et al., 2011). Extant hirsutellids include *H. scitula*, *H. hirsuta* and *H. theyeri*; genetic

480 data available for *H. hirsuta* indicate a single genotype (Schiebel and Hembleben, 2017). Modern

481 *H. scitula* and *H. hirsuta* are deep water forms. Depth habitat reconstructions show *H. scitula* at

482 the greatest water depth (Boscolo-Galazzo, Crichton et al., 2021; Fig. 1), consistent with it being

483 reported to have a deeper average depth habitat than *H. hirsuta* in the modern ocean (Birch et al.,

484 2013; Stainbank et al., 2019), where it feeds on suspended organic matter (Itou et al., 2001).

485 *Hirsutella hirsuta* has been reported to feed on dead diatoms and to predominantly live at depths

486 around 250 m (Schiebel and Hemleben, 2017), consistent with our habitat reconstructions placing

487 *H. hirsuta* and other hirsutellids shallower than *H. scitula*, between the bottom of the euphotic

488 zone and the upper twilight zone. Our depth habitat reconstruction for *H. scitula* at Site 516 for

489 the 15 Ma time slice, indicates an initial euphotic zone depth habitat preference for this species.

490 By the 7.5 Ma time slice, we find *H. scitula* at most of our low latitude sites, at depth comprised

491 between 300-500 m (Fig. 1). We suggest that the spread of *H. scitula* from high-mid latitudes

492 towards the tropics after the middle Miocene warmth (~~Figs~~Fig. 7-11) tracks increasing availability

493 of POC and oxygen at depth (Boscolo-Galazzo, Crichton et al., 2021; Fig. 12), allowing this

494 species to find food in deep tropical twilight zone waters, profiting from a new ecological niche.

495 We suggest that moving from a surface to a deep-water habitat was for *H. scitula* an ecological

496 innovation which allowed the species to move outside its high-mid latitude areal, consistent with

497 observations from the modern ocean documenting *H. scitula* dwelling at progressively deeper

498 depth from high to tropical latitudes (Schiebel and Hemleben, 2017). The proceeding ocean

499 cooling (and increasing efficiency of the biological pump) explains the stepwise depth habitat

500 increase of *H. scitula* through time at tropical and subtropical sites (Fig.1): more food became

27

501   available at increasingly greater depth in association with improved oxygen availability (Fig. 12),

502   allowing the species to expand its habitat

503
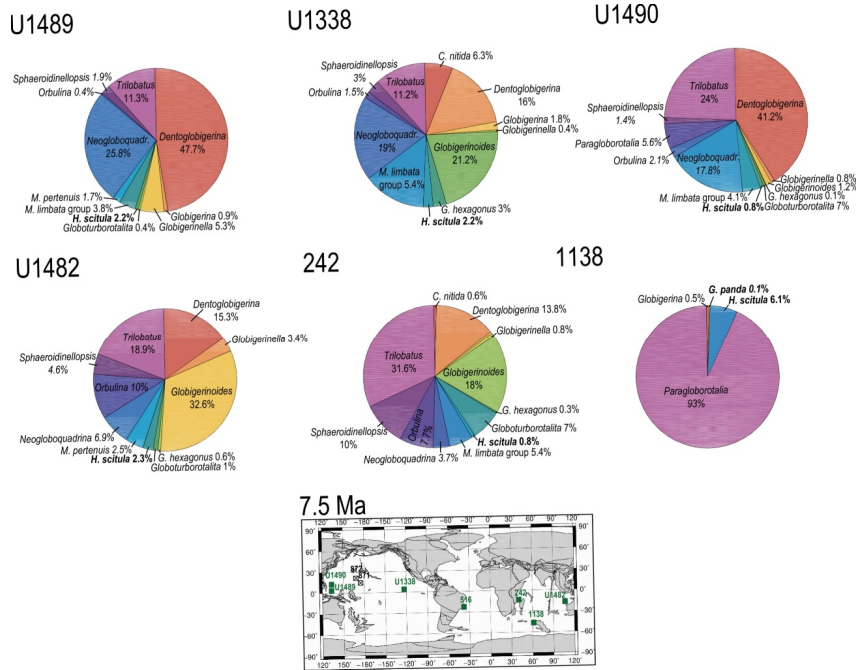
Figure 8. Abundance and biogeography of planktonic foraminiferal species at 7.5 Ma. In the pie-charts twilight zone planktonic foraminiferal species are in bold. Sites where twilight zone planktonic foraminifera were found are highlighted in green in the maps. The crossed square symbol in the maps indicate that the time interval of interest was not recovered for a given site. Continental configuration follows: Ocean Drilling Stratigraphic Network (GEOMAR, Kiel, Germany).

515

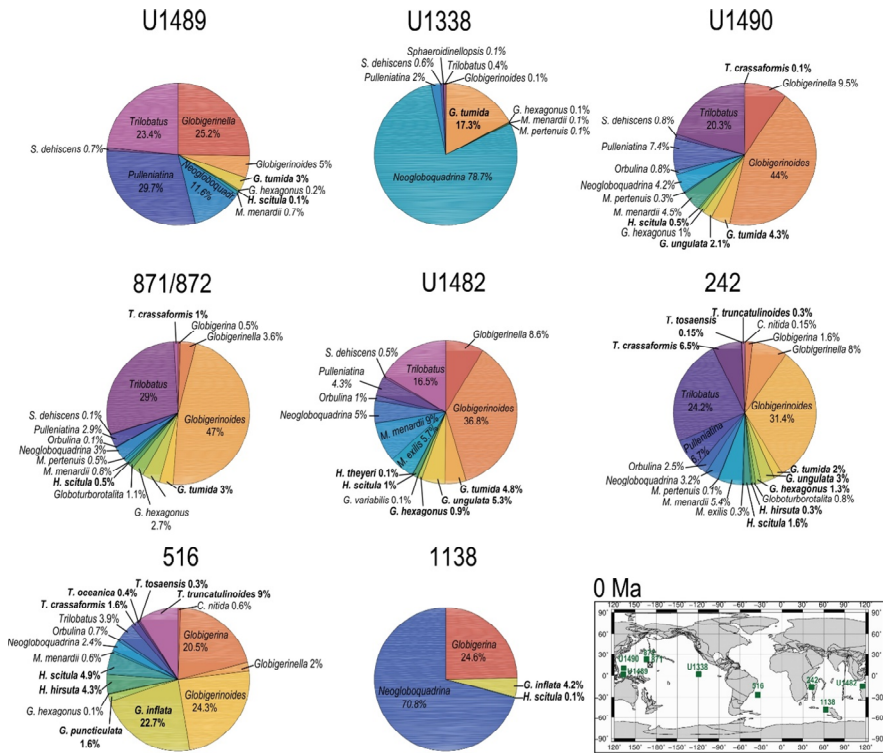**Figure 9.** Abundance and biogeography of planktonic foraminiferal species at 4.5 Ma. In the pie-charts twilight zone planktonic foraminiferal species are in bold. Sites where twilight zone planktonic foraminifera were found are highlighted in green in the maps. The crossed square symbol in the maps indicate that the time interval of interest was not recovered for a given site. Continental configuration follows: Ocean Drilling Stratigraphic Network (GEOMAR, Kiel, Germany).

527 vertically other than geographically. At low latitude sites this was accompanied by speciation, with

528 the appearance of *Hirsutella margaritae* and *H. theyeri* in the early Pliocene, and of *H. hirsuta* in

529 the Holocene. These new species display depth habitats shallower than *H. scitula* at their

530 appearance. Hence, we suggest that it was the occupation of a new deep water habitat in tropical

531 waters that triggered speciation from *H. scitula* through depth sympatry, i.e. genetic isolation

532 attained in the same area but at different depths (Weiner et al., 2012). Earlier studies on speciation

533 among planktonic foraminifera based on the fossil record, highlighted a predominance of

534 sympatric speciation, possibly linked to changes in ecology (Norris et al., 1993; Lazarus et al.,

535 1995; Pearson et al., 1997). This has more recently been supported by genetic analysis, which

536 reveals a consistent depth separation between intra-specific genotypes at a global scale, suggesting

537 that depth sympatry could be a universal mechanism generating diversity among microplankton

538 (Weiner et al., 2012).

539   Truncorotaliids start their evolutionary history at ~4.31 Ma (Raffi et al., 2020), when

540 *Truncorotalia crassaformis* splits from *Hirsutella cibaoensis* (Kennett and Srinivasan, 1983; Aze

541 et al., 2011), one of the first new species originating from *H. scitula* after its spread to low latitudes

542 (Kennett and Srinivasan, 1983). Our reconstructed geographic and temporal distribution for *T.*

543 *crassaformis* suggests that the early Pliocene split from the hirsutellids happened in cold subpolar

544 water. By the early Pliocene *Truncorotalia crassaformis* was an abundant component of the

545 subpolar assemblage at Site 1138 (>17%) and had already successfully spread to middle latitudes

546 (>8%) but does not occur in our low latitude samples (Fig.9).

547

548

549
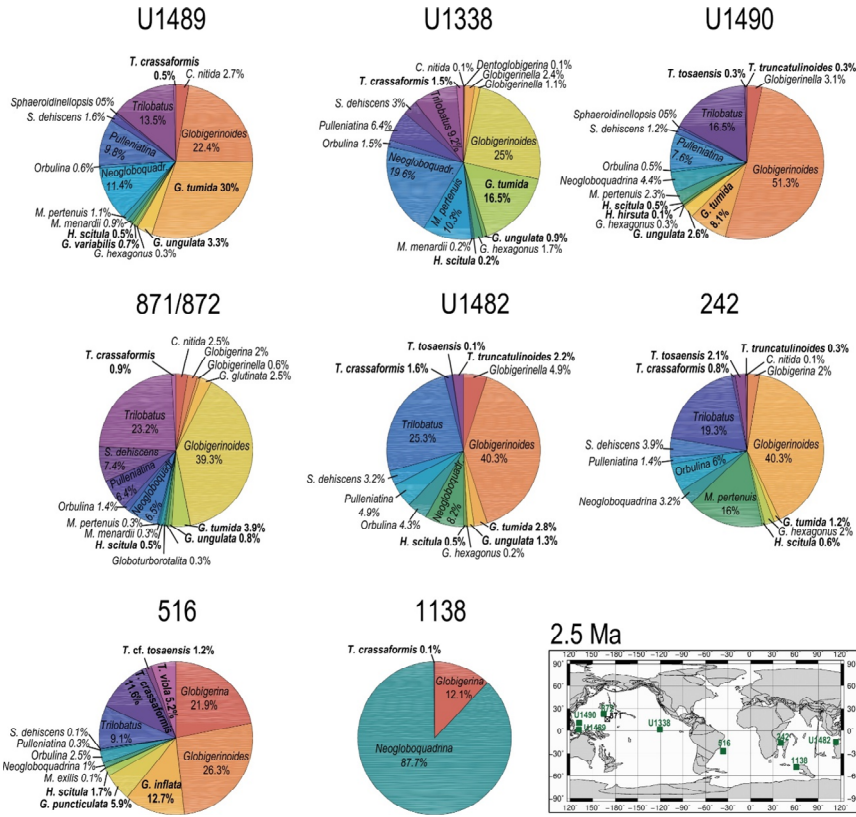
Figure 10. Abundance and biogeography of planktonic foraminiferal species at 2.5 Ma. In the pie-charts twilight zone planktonic foraminiferal species are in bold. Sites where twilight zone planktonic foraminifera were found are highlighted in green in the maps. The crossed square symbol in the maps indicate that the time interval of interest was not recovered for a given site. Continental configuration follows: Ocean Drilling Stratigraphic Network (GEOMAR, Kiel, Germany).

556

Figure 11. Abundance and biogeography of twilight zone planktonic foraminiferal species at 0 Ma. In the pie-charts twilight zone planktonic foraminiferal species are in bold. Sites where twilight zone planktonic foraminifera were found are highlighted in green in the maps. The crossed square symbol in the maps indicate that the time interval of interest was not recovered for a given site. Continental configuration follows: Ocean Drilling Stratigraphic Network (GEOMAR, Kiel, Germany).

565   Although modern planktonic foraminifera have a high dispersal potential (Darling et al., 2000;

566   Norris and De Vergas, 2000), our dataWe suggest that the evolution of *Truncorotalia crassaformis*

567   from the hirsutellids m~~ay~~ight have happened through allopatry, with low latitude population of *H.*

568   *cibaoensis* becoming isolated from subpolar populations and eventually evolving into *T.*

569   *crassaformis* (e.g., following the development of diachrony reproductive seasons in high and low

570   latitude populations). Similar to *H. scitula,* from subpolar latitudes, *Truncorotalia crassaformis*

571   appears to have subsequently spread to lower latitudes occupying progressively deeper habitats

572   (Fig. 1; ~~Figs~~Fig. 7-11), and originating numerous daughter species, some of which are intermediate

573   morphospecies with limited geographic distributions no longer extant today (Lazarus et al., 1995).

574   At Site 516 we find *Truncorotalia viola*, with lighter δ^{18}O and δ^{13}C values than *T. crassaformis*

575   (Fig. S2), pointing to a clear ecological differentiation. Together with the marked morphological

576   differentiation between the two, this suggests *T. viola* may have been a different biological species.

577   *Truncorotalia truncatulinoides*, the most representative species of this group, appears to have

578   originated from *T. crassaformis* at about 2.7 Ma in the tropical southwest Pacific, and subsequently

579   spread in the global ocean (Dowsett, 1988; Lazarus et al., 1995). According to our reconstruction,

580   depth sympatry associated with gradual morphological changes characterizes speciation among

581   the truncorotaliids, as depth habitat deepening of the ancestor/precursor is clear in the transition *T.*

582   *crassaformis-T. viola* and *T. crassaformis-T. tosaensis-T. truncatulinoides* in our record (Fig. 1).

583   The possibility to colonize deeper water habitats may have led to progressive reproductive

584   isolation between "deeper" and "shallower" populations of *T. crassaformis*, resulting in biological

585   speciation. Depth sympatry as speciation mechanism for the truncorotaliids was already proposed

586   by Lazarus et al. (1995) based on biogeography, but without a definitive test.

34

In the modern ocean the *Globorotalia merotumida-tumida* lineage is represented by *G. tumida* and *G. ungulata*, distributed in tropical to temperate regions. Genetic analysis has revealed that they are two distinct biological species with a single genotype each (Schiebel and Hemleben, 2017). Little is known about the ecology of these two species, although *G. tumida* is known to dwell in subsurface waters at the deep chlorophyll maximum (Schiebel and Hemleben, 2017). According to the phylogeny of Aze et al. (2011), *Menardella menardii* gave rise to the *Globorotalia merotumida-tumida* lineage around 9 Ma. However, *Menardella menardii* is absent in our late Miocene samples while other menardellids such *Menardella limbata* and *M. pertenuis* are common at several of our investigated middle latitudes to tropical sites. By 4.5 Ma, *Globorotalia tumida* had evolved and is common at all of our low latitude sites (Fig. 9), while *M. menardii* is extremely rare, occurring only at Sites U1338 and U1490 (0.1%), becoming more common only by the Holocene. Based on this biogeographic pattern, we propose that the *G. merotumida-tumida* lineage originated from a late Neogene menardellid, such for instance *M. limbata* which is morphologically very similar to *G. merotumida*. Given that *G. plesiotumida* and *G. tumida* display a deeper habitat (> 200 m) than *M. limbata* and other Miocene menardellids (100-200 m), we suggest that such transition may have happened through depth sympatry in tropical waters, with forms which remained reproductively isolated in the twilight zone generating the *G. merotumida-tumida* lineage. Morphometric measurements on *M. limbata* and *G. merotumida* shells are required to test for an evolutionary relationship between these two species. According to our depth habitat reconstruction, *G. plesitumida* and *G. tumida* occupied a similar depth habitat at 4.5 Ma, so it is not clear from our dataset which evolutionary mechanism may have led to the origination of the latter from the first. Hull and Norris (2009) analyzed speciation within this lineage and suggested that the evolution from *G. plesiotumida* to *G. tumida* happened

abruptly within 44 kyr. *Globorotalia ungulata*, appears in our record by the late Pliocene and often

display a habitat shallower than *G. tumida*, suggesting depth sympatry as the evolutionary

mechanism leading from *G. tumida* to *G. ungulata*. However, because depth habitat

reconstructions for these two species are more variable and shallower than that of other twilight

zone species, more data are required to more conclusively infer speciation mechanisms.

The globoconellids originated in the late early Miocene (~17 Ma) with *Globoconella*

miozea, which is considered to descend directly from *Hirsutella praescitula* (Kennett and

Srinivasan, 1983; Scott et al., 1990; Norris et al., 1994; Aze et al., 2011). *Globoconella*

conoideamiotumida originated in the middle Miocene and, after the extinction of *G. miozea* at

about 10 Ma, remained the only representative of the globoconellids until the latest Miocene. At

this time, the evolutionary turnover within the group accelerated and a number of different

morphospecies originate from *G. conoideamiotumida* and go extinct very rapidly, until the

appearance in the late Pliocene of *G. inflata* which persists until today (Wei and Kennett, 1988;

Wei, 1994; Aze et al., 2011). Compared to other Neogene to Recent taxa, the globoconellids

display a more restricted geographic distribution throughout their evolutionary history. They tend

to be common at mid latitude hydrographic fronts (Schneider and Kennett, 1999; Schiebel and

Hemleben, 2017; Lam and Leckie, 2020; Brombacher et al., 2021), except *G. puncticulata* and *G.*

inflata, which extend into low latitude regions (Norris et a., 1994). The geographic distribution of

globoconellids as shown here suggests that this group was already specialized to live at

hydrographic fronts in the middle Miocene, possibly feeding on phytoplankton. Starting at ~5.5

Ma, cooling and the possibility to feed on sinking detritus in deeper waters (Boscolo-Galazzo,

Crichton et al., 2021) may have stimulated evolutionary turnover within this otherwise rather static

group. The closely spaced temporal succession of morphospecies at this time may reflect ongoing

36

633 evolutionary experiments in an attempt to profit from new ecological possibilities opening up at

634 depth and outside the area of the group. The depth habitat reconstructions for *G. puncticulata* and

635 *G. inflata* suggests that from the Pliocene this group started
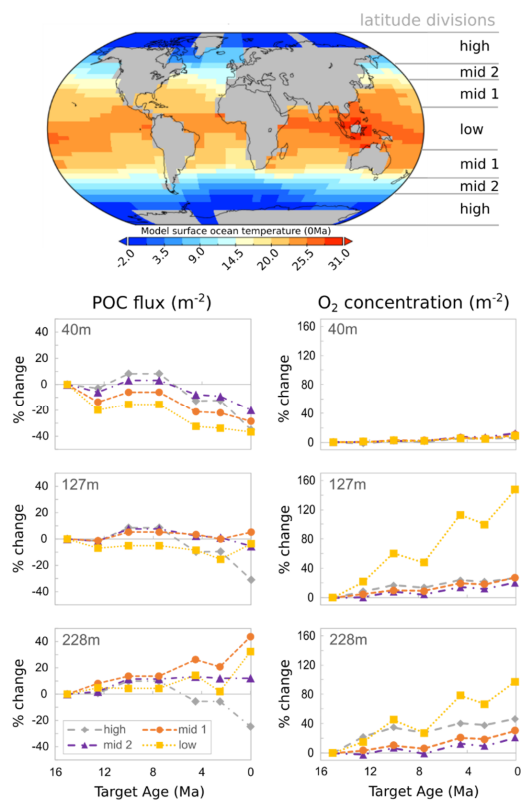
636

637 **Figure 12.** cGENIE model output for changes in Particulate Organic Carbon (POC) flux, and

638 dissolved Oxygen in near-surface ocean waters from the middle Miocene to Present, with a

639 temperature-dependent biological carbon pump. Inset map shows the modelled Present surface

640 ocean temperatures. Depths are the middle of cGENIE's top three ocean layers.

641

642 to progressively adapt to greater depths, consistent with the distinctive change in morphology

643 between *G. sphericomiozea* (and other Miocene globoconellids) and its Pliocene descendants *G.*

644 *puncticulata* and *G. inflata* (Kennett and Srinivasan, 1983), as well as with previous stable isotope

645 reconstructions for these species (Schneider and Kennett, 1996). We suggest that an evolutionary

646 transition began with the morphospecies *G. puncticulata*, transitional between *G. sphericomiozea*

647 and *G. inflata* and led to the late Pliocene speciation of *G. inflata*. It is not clear from our data

648 whether depth sympatry or allopatry allowed the speciation of *G. inflata,* as *G. puncticulata* and

649 *G. inflata* show similar depth habitat in our record. It may have been a combination of the two,

650 given *G. inflata* genotypes display a characteristic allopatric distribution in the ocean (Morard et

651 al., 2011).

652   Our data indicate that combining stable isotopes and model-derived water column temperature

653 is a promising approach to quantify the depth habitat of extinct planktonic foraminiferal species.

654 When combined with abundance and biogeographic data, depth habitat reconstructions offer

655 insights into speciation mechanisms not resolvable with the use of one technique alone (e.g., stable

656 isotopes). Our reconstructions indicate that both allopatry and depth sympatry played a role in the

657 origin of modern deep-dwelling planktonic foraminiferal species. Both allopatry and depth

658 sympatry appear to have been involved with the cladogenesis of the truncorotaliid and the

659 globorotaliid lineages, while depth sympatry seems to be mostly involved for intra-lineage

660 speciation.

661 **5. Conclusions**

662   Our global abundance and biogeographic data combined with our depth habitat

663 reconstructions allow us to piece together the environmental drivers behind speciation in two of

664 the most extensively studied group of pelagic microfossils, planktonic foraminifera and calcareous

665   nannofossils over the last 15 million years. The evolution of the new Neogene deep-water lineages

666   of the hirsutellids, globorotaliids, globoconellids and truncorotaliids, and of nannoplankton lower-

667   euphotic zone and sub-euphotic zone species, resulted in the vertical stratification of species seen

668   in the modern ocean, in particular at low latitudes. For planktonic foraminifera such vertical

669   stratification of species, hundreds of meters below the surface, originated through depth sympatry

670   as well as cladogenesis of new lineages via both sympatry and allopatry.

671   Our study places the evolution of modern plankton groups in the context of large scale

672   changes in ocean macroecology driven by the global climate dynamics of the past fifteen million

673   years. The late Miocene to present evolutionary history of planktonic foraminifera and

674   nannoplankton was linked, wherein increased efficiency of the biological pump with cooling since

675   the middle Miocene was a shared evolutionary driver. Lower rates of organic matter

676   remineralization in the upper part of the water column allowed the creation of new ecological

677   niches in deep waters, by increasing food delivery and oxygen at depth for heterotrophic planktonic

678   foraminifera, and by clearing surface waters and augmenting the concentration of macronutrients

679   at depth for nannoplankton.

680

700

701 **References**

702 Ando, A., Huber, B.T., and MacLeod, K.G.: Depth-habitat reorganization of planktonic
703 foraminifera across the Albian/Cenomanian boundary, Paleobiology, 36, 357-373, 2010.

704   Aze, T., Ezard, T.H.G., Purvis, A., Coxall, H.K., Stewart, D.R.M., Wade, B.S., and Pearson, P.N.:

705   A phylogeny of Cenozoic macroperforate planktonic foraminifera from fossil data, Biological

706   Reviews, 86, 900–927, 2011.

707   Bergen, J.A., de Kaenel, E., Blair, S.A., Boesiger, T.M., and Browning, E.: Oligocene-Pliocene

708   taxonomy and stratigraphy of the genus Sphenolithus in the circum North Atlantic Basin: Gulf of

709   Mexico and ODP Leg 154, J. Nannoplankt. Res. 37, 77–112, 2017.

710   Berggren, W.A.: Late Neogene planktonic foraminiferal biostratigraphy of the Rio Grande Rise

711   (SouthAtlantic). Mar. Micropaleontol., 2, 265-313, 1977.

712   Berggren, W.A.: Neogene planktonic foraminifer magnetostratigraphy of the southern Kerguelen

713   Plateau (Sites 747, 748, 751). In: Wise, SW; Schlich, R; et al. (eds.), Proceedings of the Ocean

714   Drilling Program, Scientific Results, College Station, TX (Ocean Drilling Program), 120, 631-647,

715   1992.

716   Birch, H., Coxall, H.K., Pearson, P.N., Kroon, D., and O'Regan, M.: Planktonic foraminifera

717   stable isotopes and water column structure: Disentangling ecological signals, Marine

718   Micropaleontology, 101, 127–145, 2013.

719   Blair, S.A., Bergen, J.A., de Kaenel, E., Browning, E., and Boesiger, T.M.: Upper Miocene-Lower

720   Pliocene taxonomy and stratigraphy in the circum North Atlantic Basin: radiation and extinction

721   of Amauroliths, Ceratoliths and the D. quinqueramus lineage, Journal of Nannoplankton Research.

722   37, 113–144, 2017

723 Boesiger, T.M., de Kaenel, E., Bergen, J.A., Browning, E., and Blair, S.A.: Oligocene to

724 Pleistocene taxonomy and stratigraphy of the genus Helicosphaera and other placolith taxa in the

725 circum North Atlantic Basin, Journal of Nannoplankton Research. 37, 145–175, 2017.

726 Bolli, H.M., Saunders, J.B., and Perch-Nielsen, K.: Plankton Stratigraphy: Volume 1, Planktic

727 Foraminifera, Calcareous Nannofossils and Calpionellids. Cambridge University Press, 599 pp.,

728 1989.

729 Boscolo-Galazzo, F., Crichton, K.A., Ridgwell, A., Mawbey, E.M., Wade, B.S., and Pearson P.N.:

730 Temperature controls carbon cycling and biological evolution in the ocean twilight zone, Science,

731 371, 1148–1152, 2021.

732 Bown, P.R., and Young, J.R, Techniques. In: P.R. Bown (Ed.). Calcareous Nannofossil

733 Biostratigraphy, British Micropalaeontological Society Publications Series/Kluwer Academic,

734 London, 16–28 pp., 1998.

735 Bown, P.R., Lees, J.A., and Young, J.R.: Calcareous nannoplankton evolution and diversity

736 through time. In: H.R. Thierstein and J.R. Young (Editors), Coccolithophores: From Molecular

737 Processes to Global Impact. Springer, Berlin, 481-508, 2004.

738 Brombacher, A., Wilson, P.A., Bailey, I., and Ezard, T.H.: The Dynamics of Diachronous

739 Extinction Associated with Climatic Deterioration near the Neogene/Quaternary Boundary,

740 Paleoceanography and Paleoclimatology, e2020PA004205, 2021.

741 Browning, E., de Kaenel, E., Bergen, J.A., Blair, S.A., and Boesiger, T.M.: Oligocene-Pliocene

742 taxonomy and stratigraphy of the genus *Sphenolithus* in the circum North Atlantic Basin: Gulf of

743 Mexico and ODP Leg 154, Journal of Nannoplankton Research, 37, 77–112, 2017.

Ciummelli, M., Raffi, I., and Backman, J.: Biostratigraphy and evolution of Miocene Discoaster spp. from IODP Site U1338 in the equatorial Pacific Ocean, J. Micropalaeontology, 36, jmpaleo2015-034, 2016.

Coxall, H.K., Wilson, P.A., Pearson, P.N., and Sexton, P.F.: Iterative evolution of digitate planktonic foraminifera. Paleobiology, 33, 495–516, 2007.

Cramer, B.S., Miller, K.G., Barrett P.J., and Wright, J.D.: Late Cretaceous–Neogene trends in deep ocean temperature and continental ice volume: Reconciling records of benthic foraminiferal geochemistry (d18O and Mg/Ca) with sea level history. J. Geophys. Res., 116, C12023, 2011.

Crichton K.A., Ridgwell A., Lunt D.J., Farnsworth A., and Pearson P.N.: Data-constrained assessment of ocean circulation changes since the middle Miocene in an Earth system model. Clim. Past https://doi.org/10.5194/cp-2019-151, 2020.

Crichton, K.A., Wilson, J.D., Ridgwell, A., and Pearson P.N.: Calibration of key temperature-dependent ocean microbial processes in the cgenie.muffin Earth system model, Geosciences Model Development, 14, 125–149, 2021.

Darling, K.F., Christopher, M.W., Stewart, I.A., Kroon, D., Dinglek, R. and Leigh Brown A.J., Molecular evidence for genetic mixing of Arctic and Antarctic subpolar populations of planktonic foraminifers, Nature, 405, 43-47, 2000.

De Kaenel, E., Bergen, J.A., Browning, E., Blair, S.A., and Boesiger, T.M.: Uppermost Oligocene to Middle Miocene Discoaster and Catinaster taxonomy and stratigraphy in the circum North Atlantic Basin: Gulf of Mexico and ODP Leg 154, Journal of Nannoplankton Research, 37, 77–112, 2017.

765 De Vargas, Renaud, C.S., Hilbrecht, H., and Pawlowski, J.: Pleistocene adaptive radiation in

766 Globorotalia truncatulinoides: genetic, morphologic, and environmental evidence, Paleobiology,

767 27, 104–125, 2001.

768 Davis, C.V., Wishner, K., Renema, W., and Hull, P.M.,: Vertical distribution of planktic

769 foraminifera through an oxygen minimum zone: how assemblages and test morphology reflect

770 oxygen concentrations, Biogeosciences, 18, 977–992, 2021.

771 Dowsett, H.J.: Diachrony of late Neogene microfossils in the Southwest Pacific Ocean: application

772 of the graphic correlation method, Paleoceanography, 3, 209-222, 1988.

773 Ezard, T.H.G., Aze, T., Pearson, P.N., and Purvis, A.: Interplay Between Changing Climate and

774 Species' Ecology Drives Macroevolutionary Dynamics, Science, 332, 349-351, 2011.

775 Fox, L.R., and Wade, B.S.: Systematic taxonomy of early–middle Miocene planktonic

776 foraminifera from the equatorial Pacific Ocean: Integrated Ocean Drilling Program, Site U1338,

777 The Journal of Foraminiferal Research 43, 374-405, 2013.

778 Fraass, A.J., Kelly, D.C., and Peters, S.E.: Macroevolutionary History of the Planktic

779 Foraminifera, Annu. Rev. Earth Planet. Sci., 431, 39–66, 2015.

780 Godrijan, J., Drapeau, D., and Balch, W.M.: Mixotrophic uptake of organic compounds by

781 coccolithophores, Limnology and Oceanography 00, 1–12, 2020.

782 Gibbs, S.J., Bown, P.R., Ward, B.A., Alvarez, S.A., Kim, H., Archontikis, O.A., Sauterey, B.,

783 Poulton, A.J., Wilson, J., and Ridgwell, A.: Algal plankton turn to hunting to survive and recover

784 from end-Cretaceous impact darkness, Sci. Adv. 6, eabc9123, 2020.

785 Greco, M., Jonkers, L., Kretschmer, K., Bijma, J., and Kucera, M.: Depth habitat of the planktonic

786 foraminifera Neogloboquadrina pachyderma in the northern high latitudes explained by sea-ice

787 and chlorophyll concentrations, Biogeosciences, 16, 3425–3437, 2019.

788 Hammer, Ø., Harper, D.A.T., and Ryan, P.D.: PAST: Paleontological Statistics Software Package

789 for Education and Data Analysis, Palaeontologia Electronica 4, 9 pp., 2001.

790 Henderiks, J., Bartol, M., Pige, N., Karatsolis, B.-T., and Lougheed, B.C.: Shifts in phytoplankton

791 composition and stepwise climate change during the middle Miocene, Paleoceanography and

792 Paleoclimatology, 35, e2020PA003915, 2020.

793 Herbert, T.D., Lawrence, K.T., Tzanova, A., Peterson, L.C., Caballero-Gill, R., and Kelly, C.S.:

794 Late Miocene global cooling and the rise of modern ecosystems. Nature Geoscience, 9, 843–847,

795 2016.

796 Hodell, D.A. and Vayavananda, A.: Middle Miocene paleoceanography of the western equatorial

797 Pacific (DSDP Site 289) and the evolution of Globorotalia (Fohsella), Marine Micropaleontology,

798 22, 279–310, 1993.

799 Hull P.M., and Norris R.D.: Evidence for abrupt speciation in a classic case of gradual evolution,

800 PNAS, 106, 21224–21229, 2009.

801 Hull, P. M., Osborn, K. J., Norris, R. D., and Robison, B. H.: Seasonality and depth distribution

802 of a mesopelagic foraminifer, Hastigerinella digitata, Monterey Bay, California, Limnol.

803 Oceanogr., 56, 562–576, 2011.

45

804 Itou, M., Ono, T., Olba, T., and Noriki, S.: Isotopic composition and morphology of living
805 Globoborotalia scitula: a new proxy of sub-intermediate ocean carbonate chemistry? Marine
806 Micropaleontology, 42, 189-210, 2001.

807 Jenkins, D.G. and Srinivasan, M.S.: Cenozoic planktonic foraminifers from the equator to the sub-
808 antarctic of the southwest Pacific, In: Kennett, J.P., von der Borch, C.C., Baker, P.A., Barton, C.E.,
809 Boersma, A., Caulet, J.P., et al., (Eds), Initial Reports of the Deep Sea Drilling Project 90, 795–
810 834, 1986.

811 John, E.H., P.N. Pearson, H.K. Coxall, H. Birch, B.S. Wade, and Foster G.L.: Warm ocean
812 processes and carbon cycling in the Eocene, Philos. Trans. R. Soc. A, doi:10.1098/rsta.2013.0099,
813 2013.

814 Jones, A.P., Dunkley Jones, T., Coxall, H., Pearson, P.N., Nala, D. and Hoggett, H.: Low-latitude
815 calcareous nannofossil response in the Indo-Pacific Warm Pool across the Eocene–Oligocene
816 Transition of Java, Indonesia. Paleoceanography and Paleoclimatology, 34, 1–15, 2019

817 Jonkers, L., and Kucera, M.: Global analysis of seasonality in the shell flux of extant planktonic
818 Foraminifera, Biogeosciences, 12, 2207–2226, 2015.

819 Kennett, J.P., and Srinivasan, M.S.: Neogene Planktonic Foraminifera. Hutchinson Ross
820 Publishing Co., Stroudsburg, Pennsylvania, 1-265 pp, 1983.

821 Kennett, J.P., and Von der Borch, C.C.: Southwest Pacific Cenozoic Paleoceanography. In
822 Kennett, J.P., von der Borch, C.C., et al., Initial Reports of the Deep Sea Drilling Project, 90:
823 Washington, DC (U.S. Government Printing Office), 1493–1517, 1986.

824 Kennett, J.P., and Exon, N.F.: Palaeoceanographic Evolution of the Tasmanian Seaway and its

825 Climatic Implications, In: Exon, N.F., Kennett, J.P., and Malone, M.J. (Eds.), The Cenozoic

826 Southern Ocean: Tectonics, Sedimentation, and Climate Change between Australia and

827 Antarctica. Geophysical Monograph, 151, 345–367, 2004.

828 Kim S.-T., and O'Neil J.R.: Equilibrium and non-equilibrium oxygen isotope effects in synthetic

829 carbonates. Geochim. Cosmochim. Acta, 61, 3461–3475, 1997.

830 Kucera, M., and Schonfeld, J.: The origin of modern oceanic foraminiferal faunas and Neogene

831 climate change, in Williams, M., Haywood, A.M., Gregory, F.J. and Schmidt, D.N. (eds) Deep-

832 Time Perspectives on Climate Change: Marrying the Signal from Computer Models and Biological

833 Proxies. The Micropalaeontological Society, Special Publications, The Geological Society,

834 London, 409–425, 2007.

835 Lam A.R., and Leckie R.M.: Late Neogene and Quaternary diversity and taxonomy of subtropical

836 to temperate planktic foraminifera across the Kuroshio Current Extension, northwest Pacific

837 Ocean, Micropaleontology, 66, 177–268, 2020a.

838 Lam, A. R., and Leckie, R. M.: Subtropical to temperate late Neogene to Quaternary planktic

839 foraminiferal biostratigraphy across the Kuroshio Current Extension, Shatsky Rise, northwest

840 Pacific Ocean, PLoS ONE, 15, e0234351, 2020b.

841 Lazarus, D.B., Hilbrecht, H., Spencer-Cervato, C. and Thierstein, H.: Sympatric speciation and

842 phyletic change in Globorotalia truncatulinoides, Paleobiology, 21, 28–51, 1995.

843 Lowery, C.M., Bown, P.R., Fraass, A.J. and Hull, P.M.,: Ecological Response of Plankton to
844 Environmental Change: Thresholds for Extinction, Annual Review of Earth and Planetary
845 Sciences, 48, 403-429, 2020.

846 Matsui, H., Nishi, H., Takashima, R., Kuroyanagi, A., Ikehara, M., Takayanagi, H., and Iryu, Y.:
847 Changes in the depth habitat of the Oligocene planktic foraminifera (Dentoglobigerina
848 venezuelana) induced by thermocline deepening in the eastern equatorial Pacific,
849 Paleoceanography, 31, 715-731, 2016.

850 Majewski, W.: Planktonic Foraminiferal Response to Middle Miocene Cooling in the Southern
851 Ocean (ODP Site 747, Kerguelen Plateau), Acta Palaeontologica Polonica, 55, 541-560, 2010.

852 Meilland, J., Siccha, M., Weinkauf, M. F. G., Jonkers, L., Morard, R., Baranowski, U., Baumeister,
853 A., Bertlich, J., Brummer, G. J., Debray, P., Fritz-Endres, T., Groeneveld, J., Magerl, L., Munz,
854 P., Rillo, M. C., Schmidt, C., Takagi, H., Theara, G., and Kucera, M.: Highly replicated sampling
855 reveals no diurnal vertical migration but stable species-specific vertical habitats in planktonic
856 foraminifera, J. Plank. Res., 41, 127–141, 2019.

857 Morard, R., Quillevere, F., Douady, C.J., De Vargas, C., De Garidel-Thoron, T., and Escarguel,
858 G.: Worldwide Genotyping in the Planktonic Foraminifer Globoconella inflata: Implications for
859 Life History and Paleoceanography, PLoS ONE 6(10): e26665, 2011.

860 Norris, R., D.: Pelagic Species Diversity, Biogeography, and Evolution, Paleobiology, 26, 236-
861 258, 2000.

862 Norris, R.D., and Corfield, R.M.: Evolutionary ecology of Globorotalia (Globoconella) (planktic
863 foraminifera), Marine Micropaleontology, 23, 121–145, 1994.

48

864 Norris, R.D. and de Vargas, C.: Evolution all at sea, Nature, 405, 23-24, 2000.

865 Norris, R.D., Corfield, R.M. and Cartlidge, J.E.: Evolution of depth ecology in the planktic

866 foraminifera lineage Globorotalia (Fohsella). Geology, 21, 975–978, 1993.

867 Norris, R. D., Kirtland Turner, S., Hull, P. M., and Ridgwell, A.: Marine Ecosystem Responses to

868 Cenozoic Global Change, Science, 341, 492-498, 2013.

869 ~~Morard, R., Quillevere, F., Douady, C.J., De Vargas, C., De Garidel-Thoron, T., and Escarguel,~~

870 ~~G.: Worldwide Genotyping in the Planktonic Foraminifer Globoconella inflata: Implications for~~

871 ~~Life History and Paleoceanography, PLoS ONE 6(10): e26665, 2011.~~Pearson, P.N.: Planktonic

872 foraminifer biostratigraphy and the development of pelagic caps on guyots in the marshall islands

873 group, In: Haggerty, J.A., Premoli Silva, I., Rack, R., and McNutt, M.K. (Eds.), Proceedings of

874 the Ocean Drilling Program, Scientific Results, 144, 21-59, 1995.

875 Pearson, P.N., and Coxall, K.H.: Origin of the Eocene planktonic foraminifer Hantkenina by

876 gradual evolution, Palaeontology 57, 243–267, 2012.

877 Pearson, P.N., N.J. Shackleton, and Hall M.A.: Stable isotopic evidence for the sympatric

878 divergence of Globigerinoides trilobus and Orbulina uniriersa (planktonic foraminifera), Journal

879 of the Geological Society, 154, 295-302, 1997.

880 Quillevere F., Norris R.D., Moussa I., and Berggren W.A.: Role of photosymbiosis and

881 biogeography in the diversification of early Paleogene acarininids (planktonic foraminifera),

882 Paleobiology, 27, 311–326, 2001.

883 Quinn, P.S., Cortés, M.Y. and Bollmann, J.: Morphological variation in the deep ocean-dwelling

884 coccolithophore Florisphaera profunda (Haptophyta), European Journal of Phycology, 40, 123-

885 133, 2005.

886 Raffi, I., Wade, B.S., Pälike, H., Beu, A.G., Cooper, R., Crundwell, M.P., Krijgsman, W., Moore,

887 T., Raine, I., Sardella, R., and Vernyhorova, Y.V.: Chapter 29 - The Neogene Period, Editor(s):

888 Felix M. Gradstein, James G. Ogg, Mark D. Schmitz, Gabi M. Ogg, Geologic Time Scale 2020,

889 Elsevier, 1141-1215 pp., 2020

890 Rebotim, A., Voelker, A. H. L., Jonkers, L., Waniek, J. J., Meggers, H., Schiebel, R., Fraile, I.,

891 Schulz, M., and Kucera, M.: Factors controlling the depth habitat of planktonic foraminifera in the

892 subtropical eastern North Atlantic, Biogeosciences, 14, 827–859, 2017.

893 Schiebel, R., and Hemleben, C.: Planktic Foraminifers in the Modern Ocean, Springer-Verlag,

894 Berlin Heidelberg, 2017.

895 Schiebel R., Smart S.M., Jentzen A., Jonkers L., Morard R., Meilland J., Michel E., Coxall H.K.,

896 Hull P.M., De Garidel-Thoron T., Aze T., Quillévéré F., Ren H., Sigman D.M., Vonhof H.B.,

897 Martínez-García A., Kucera M., Bijma J., Spero H.J., and Haug G.H., Advances in planktonic

898 foraminifer research: New perspectives for paleoceanography, Revue de micropaléontologie, 61,

899 113–138, 2018.

900 Schneider, C., and Kennett, J.: Isotopic evidence for interspecies habitat differences during

901 evolution of the Neogene planktonic foraminiferal clade Globoconella, Paleobiology, 22, 282-303,

902 1996.

903 Schneider, C., and Kennett, J.: Segregation and speciation in the Neogene planktonic foraminiferal
904 clade Globoconella, Paleobiology, 25, 383-395, 1999.

905 Scott, G.H., Bishop, S., and Burt, B.J.: Guide to some Neogene Globorotalids (Foraminiferida)
906 from New Zealand. New Zealand Geological Survey Paleontological Bulletin 61, Lower Hutt,
907 New Zealand, 176 pp., 1986.

908 Scott, G.H., Bishop, S., and Burt, B.J.: Guide to some Neogene Globorotalids (Foraminiferida)
909 from New Zealand. New Zealand Geological Survey Paleontological Bulletin 61, Lower Hutt,
910 New Zealand, 176 pp., 1990.

911 Sosdian, S.M., Greenop, R., Hain, M.P., Foster, G.L., Pearson, P.N., and Lear, C.H.: Constraining
912 the evolution of Neogene ocean carbonate chemistry using the boron isotope pH proxy, Earth and
913 Planetary Science Letters, 498, 362–376, 2018.

914 Spezzaferri, S., Kucera, M., Pearson, P.N., Wade, B.S., Rappo, S., Poole, C.R., Morard, R.,
915 Stalder, C.: Fossil and genetic evidence for the polyphyletic nature of the planktonic foraminifera"
916 Globigerinoides", and description of the new genus Trilobatus, PLoS One 10, e0128108, 2015.

917 Stainbank, S., Kroon, D., Ruggeberg, A., Raddatz, J., de Leau, E.S., Zhang, M., and Spezzaferri,
918 S.: Controls on planktonic foraminifera apparent calcification depths for the northern equatorial
919 Indian Ocean, PLoS ONE, 14, e0222299, 2019.

920 Styzen, M.J.. Cascading counts of nannofossil abundance, Journal of Nannoplankton Research,
921 19, 49, 1997.

922   Super, J.R., Thomas, E., Pagani, M., Huber, M., O'Brien, C.L., and Hull, P. M.: Miocene evolution

923   of North Atlantic Sea surface temperature. Paleoceanography and Paleoclimatology, 35,

924   e2019PA003748, 2020.

925   Wade, B.S., Pearson, P.N. Berggren, W.A. and Palike, H.: Review and revision of Cenozoic

926   tropical planktonic foraminiferal biostratigraphy and calibration to the geomagnetic polarity and

927   astronomical time scale, Earth-Science Reviews, 104, 111–142, 2011.

928   Wade, B.S., Pearson, P.N., Olsson, R.K., Fraass, A. Leckie, R.M. and Hemleben, Ch.: Taxonomy,

929   biostratigraphy, and phylogeny of Oligocene and lower Miocene Dentoglobigerina and

930   Globoquadrina, in Wade, B.S., Olsson, R.K., Pearson, P.N., Huber, B.T. and Berggren, W.A.,

931   Atlas of Oligocene Planktonic Foraminifera, Cushman Foundation of Foraminiferal Research,

932   Special Publication, No. 46, p. 331-384, 2018.

933   Wei, K.Y.: Stratophenetic tracing of phylogeny using SIMCA pattern recognition technique: A

934   case study of the late Neogene planktic foraminifera Globoconella clade, Paleobiology, 20, 52-65,

935   1994.

936   Wei, K.Y., and Kennett, J.P.: Taxonomic evolution of Neogene planktonic foraminifera and

937   paleoceanographic relations, Paleoceanography, 1, 67-84, 1986.

938   Wei, K.Y., and Kennett, J.: Phyletic gradualism and punctuated equilibrium in the late Neogene

939   planktonic foraminiferal clade Globoconella, Paleobiology, 14, 345-363, 1988.

940   Weiner, A., Aurahs, R., Kurasawa, A., Kitazato, H., and Kucera, M.: Vertical niche partitioning

941   between cryptic sibling species of a cosmopolitan marine planktonic protest, Mol. Ecol., 21, 4063–

942   4073, 2012.

943 Woodhouse, A., Jackson, S.L., Jamieson, R.A., Newton, R.J., Sexton, P.F., and Aze, T.: Adaptive

944 ecological niche migration does not negate extinction susceptibility. Scientific Reports, 11, 15411,

945 2021.

946 Young, J.R., Bergen, J.A., Bown, P.R., Burnett, J.A., Fiorentino, A., Jordan, R.W., Kleijne, A.,

947 van Niel, B.E., Romein, A.J.T. and Von Salis, K.: Guidelines for coccolith and calcareous

948 nannofossil terminology, Palaeontology, 40, 875–912, 1997.

949 Zhang, Y.G., Pagani, M., Liu Z.: A 12-Million-Year Temperature History of the Tropical Pacific

950 Ocean, Science, 344, 84-87, 2014.

951 Zenodo DOI: 10.5281/zenodo.4469673.

952 Zenodo DOI: 10.5281/zenodo.4469678.